THE MICRO-MECHANISMS OF FATIGUE DEFORMATION IN NIMONIC PE16

C.H.D. Arbuthnot

T.E.M. examination of fatigue damage in Nimonic PE16 shows that, at low strains, deformation is restricted to discrete slip-bands, whose spacing is inversely proportional to the applied plastic strain amplitude. At higher strains, the interaction of densely packed slip-bands leads to the breakdown of planar slip. This transition is accompanied by the onset of cyclic work hardening and a change in the Coffin-Manson exponent, α.

INTRODUCTION

Although many fatigue resistant alloys deform by planar slip, it is not clear whether their fatigue properties are improved by the slip character per se. Planar slip associated with shearable coherent precipitates (e.g. θ'', γ') results in lower fatigue lives than wavy slip materials or over-aged microstructures (1). However easily reversible deformation mechanisms, such as twinning, have superior fatigue properties compared to alloys which deform by wavy slip (2).

This paper describes an investigation of the deformation structures formed during low cycle fatigue testing of a γ' hardened superalloy, Nimonic PE16, over a range of plastic strain amplitudes. The effect of slip character on crack initiation and fatigue endurance is discussed.

EXPERIMENTAL

Material

Fatigue specimens were machined from a 1 inch diameter rolled bar of Nimonic PE16 whose composition is shown in Table 1.

TABLE 1 - Composition of Nimonic PE16 (wt%)

C	Si	Mn	5ppm	Al	B	Co	Cr	Mo	Ni	Ti	Zr	Fe
.067	.05	.04	12	1.19	.04	.03	16.5	3.3	43.3	1.4	.03	34.0

Heat-treatment

Specimens were solution treated at 1040^{o}C for 4 hours, followed by ageing above the γ' solvus for 1 hour, to re-precipitate $M_{23}C_6$ as discrete particles

and prevent grain boundary films forming during further ageing treatments. Finally γ' was precipitated by ageing at 750°C. Peak hardness was attained after 8-10 hours at this temperature. The γ' distribution is shown in Fig.(1).

RESULTS

Mechanical behaviour

S-N curves are shown for two different plastic strain amplitudes in Fig.(2). Specimen A, fatigued at an ΔEp of 0.56%, showed rapid cyclic softening followed by a more gradual decrease in stress amplitude throughout its life. Specimen B, fatigued at a ΔEp of 3.1% behaved similarly apart from an initial period of cyclic hardening in the first few cycles of the test. The rate of work softening as a function of cumulative plastic strain, ($d\Delta\sigma / d(N\Delta Ep)$), is approximately constant for both strain amplitudes.

The stress amplitude at half-life is plotted against plastic strain amplitude in Fig.(3). At low strains the material shows an approximately constant saturation stress irrespective of the applied strain amplitude. Above a ΔEp of 2.2% pronounced cyclic work hardening occurs.

A similar discontinuity is shown in a Coffin-Manson plot, Fig.(4), of cycles to failure against plastic strain amplitude. The slope, α, changes from 0.98 to 0.29 at a ΔEp of 2.3%, indicating that the material's fatigue endurance is less sensitive to plastic strain amplitude at higher imposed strains.

TEM investigation of deformation structures

Fig.(5) shows that the slip band density immediately after the rapid softening stage is marginally higher than during the rest of the fatigue life. A few slip-bands with a lower dislocation density than average, appear to have become redundant as plastic deformation has concentrated in bands, which have undergone more extensive cyclic softening. However, the dislocation density in the active slip-bands remains more or less constant indicating that fatigue deformation does not result in the progressive accumulation of dislocation debris.

Dislocation structures characteristic of different plastic strain amplitudes shown in Figs. (6) to (7) are described below.

ΔEp = 0.56%. Plastic deformation is entirely restricted to discrete slip-bands, apart from a few stray dislocation pairs. Most of the dislocations in slip-bands are too closely spaced (<50nm) to be resolved individually, although several are visible at A. The thin lines crossing the slip-band at B are in fact {111} planes viewed end on. The foil can be tilted so that the slip-bands show no residual contrast, indicating that the dislocations are primarily screw in character.

ΔEp = 1.55%. Two well-defined slip systems are present, forming a regular array of evenly spaced slip-bands. The spacing between slip-bands has decreased with increasing plastic-strain amplitude. Dislocation tangles are visible at the junction of several slip-bands.

ΔEp = 2.58%. Fig. (7) shows a dense array of intersecting slip-bands. Plastic deformation is still restricted to slip-bands, although a minimum spacing ($\sim 2\mu m$) has been reached.

$\Delta Ep = 4.46\%$. The slip-bands are no longer so well-defined. An increase in dislocation density indicates that deformation is no longer restricted entirely to slip-bands.

Fig. (8) shows the reciprocal slip-band spacing is inversely proportional to ΔEp up to 2.2%. The shear displacement in each band calculated from the slope of Fig.(8) is 22nm.

DISCUSSION

The most striking feature of the fatigue behaviour of Nimonic PE16 is the constant stress amplitude shown by this material over a wide range of imposed plastic strain amplitudes. The stress amplitude is governed by the internal shear stress necessary to produce a given macroscopic plastic deformation. Hence the saturation stress can be identified with the internal stress necessary to operate a slip-band. As the resultant shear displacement in each band is constant, it is not altogether surprising that the stress amplitude is also independent of plastic strain amplitude over much of the cyclic stress-strain curve.

The onset of cyclic hardening at a plastic strain amplitude of 2.2% coincides with the formation of slip-bands on three different systems, effectively limiting the mean free path of the pile-up dislocations. The slip-band structure gives way to more homogeneous deformation (Fig. 7) when the stress necessary to cause deformation in a slip-band is sufficient to operate new dislocation sources within the grain.

Since slip-band structures change very little throughout the fatigue life of a specimen, and there is no evidence of the accumulation of microstructural damage, failure must be caused by the growth of surface microcracks. Tomkins (3) has proposed a continuum model of this process based on the decohesion of intense shear bands at the crack tip. The amount of crack growth per cycle is limited by the material's cyclic hardening behaviour. The model predicts that the Coffin-Manson exponent α, and the cyclic work hardening exponent β are related by the equation:-

$$\alpha' = \frac{1}{1+2\beta}$$

Table 2 shows the predicted values for α' are in good agreement with experiment.

TABLE 2 - Experimental and Predicted values of α

β	α	α' (= $1/1+2\beta$)
0	0.98	1
0.625	0.295	0.317

However it is unlikely that a continuum model will give an accurate prediction of the fatigue behaviour of a polycrystalline material, unless the grain-boundaries present little or no obstruction to crack growth.

SEM examination of the gauge length of fatigue specimens shows that micro-cracks form in the initial stages of the test. Fig.(9) shows slip-band cracks after 5% and 30% of the total fatigue life. The high density of slip-band micro-cracks compared to larger cracks extending over several grains suggests

that most of the fatigue life is spent propagating slip-band cracks into neighbouring grains. The crack path in Fig.(10) consists of sections of inter-granular crack connecting possibly pre-existing micro-cracks across slip-bands.

At low strain amplitudes crack initiation will be favoured by high internal stresses at the intersection of slip-bands. These are absent at higher strain amplitudes and cracks tend to initiate on grain or twin boundaries, Fig.(11). The absence of slip-band cracks extending across a complete grain would be expected to seriously impede micro-crack growth and may account for the decrease in the Coffin-Manson exponent at higher strains.

CONCLUSION

The low cycle fatigue behaviour of Nimonic PE16 can be divided into two distinct regions:-

I. $\Delta Ep < 2.2\%$

Deformation restricted to slip-bands.
Cyclic work hardening exponent = 0.
Cracks initiate between slip-bands and at the intersection of slip-bands.
Coffin-Manson exponent = 0.98.

II. $\Delta Ep > 2.2\%$

Homogeneous deformation.
Pronounced cyclic work-hardening.
Micro-cracks form at grain boundaries.
Coffin-Manson exponent = 0.29.

The restriction of deformation to slip-bands has been shown to have a deleterious effect on fatigue endurance. It is uncertain whether this is due to a change in crack initiation sites or to the absence of cyclic work-hardening.

REFERENCES

1. C. Calabrese and C. Laird, Met. Trans. 5, 1785 (1978)
2. D. Fournier and A. Pineau, Met. Trans. 8A, 1095 (1977)
3. B. Tomkins, Phil. Mag. 18 p.1041 (1968)

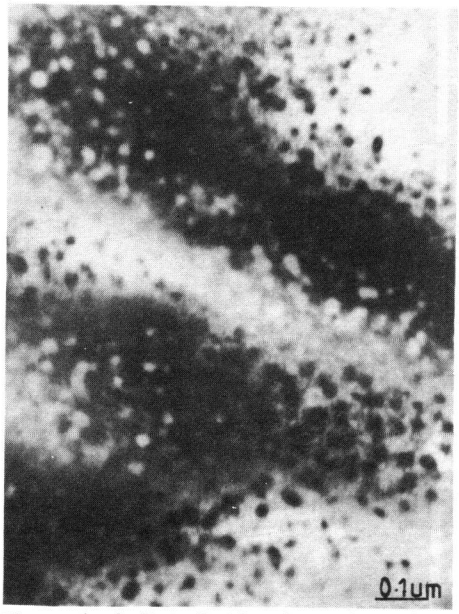

Figure 1 γ' distribution in peak aged Nimonic PE16

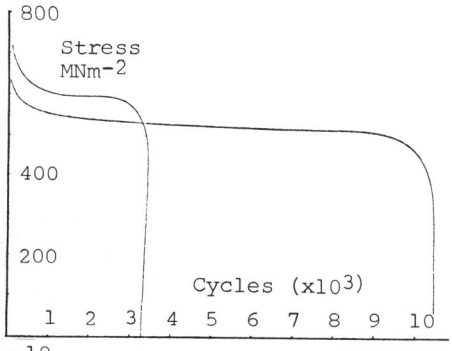

Figure 2 S-N curves

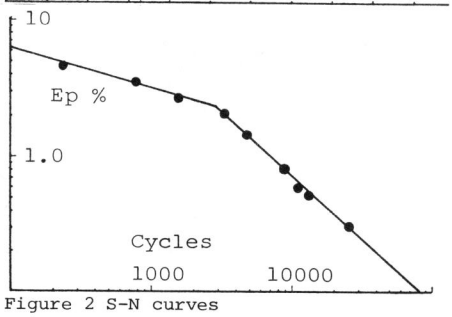

Figure 3 Coffin-Manson plot

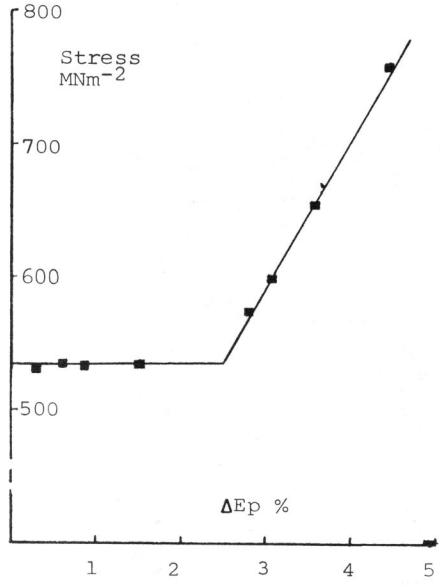

Figure 4 Cyclic stress-strain curve

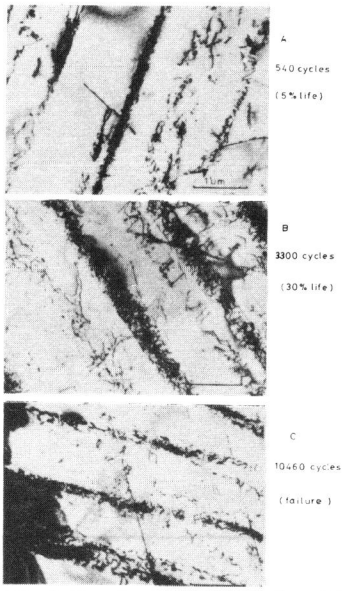

Figure 5 Development of dislocation structures throughout fatigue life

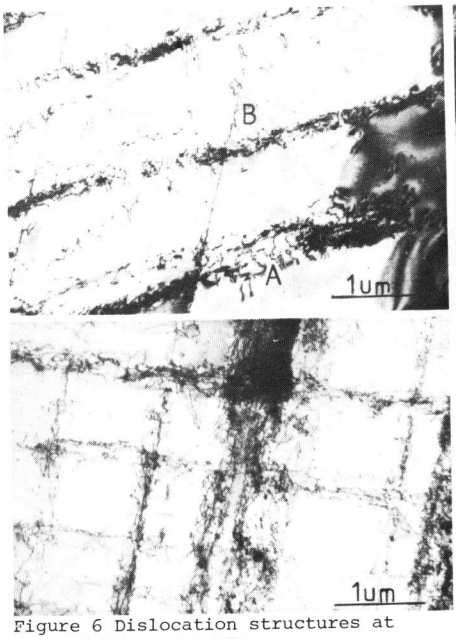

Figure 6 Dislocation structures at ΔEp = 0.56% and 1.55%

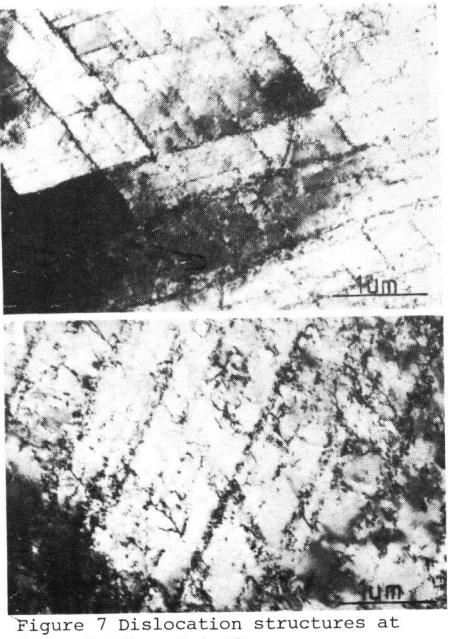

Figure 7 Dislocation structures at ΔEp = 2.58% and 4.46%

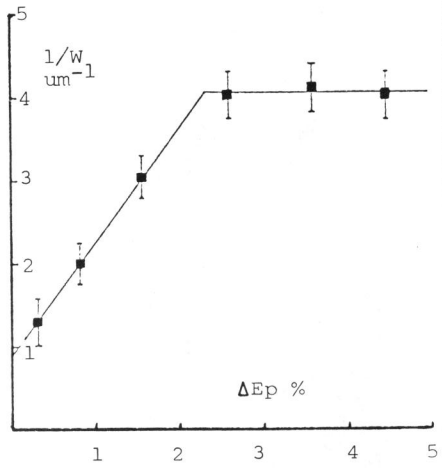

Figure 8 Reciprocal slip-band spacing vs. plastic strain amplitude

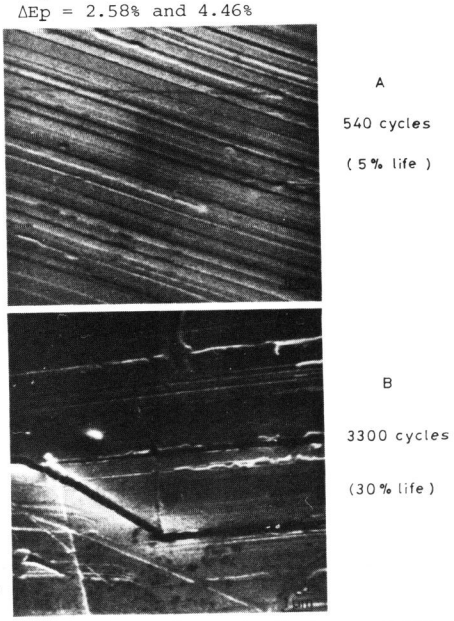

Figure 9 Development of micro-cracks during fatigue life

Figure 10 Fatigue crack showing intergranular and transgranular paths

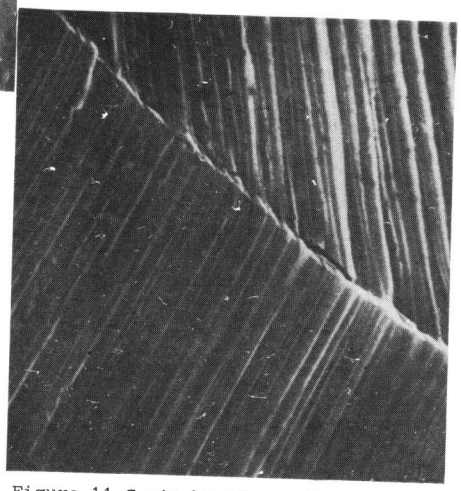

Figure 11 Grain boundary micro-crack initiation at high strain amplitudes